



Why Surface Nanobubbles Live for Hours

Joost H. Weijs and Detlef Lohse

*Physics of Fluids Group, MESA+ Institute for Nanotechnology, J. M. Burgers Centre for Fluid Dynamics, University of Twente,
P. O. Box 217, 7500 AE Enschede, The Netherlands*

(Received 20 September 2012; published 31 January 2013)

We present a theoretical model for the experimentally found but counterintuitive exceptionally long lifetime of surface nanobubbles. We can explain why, under normal experimental conditions, surface nanobubbles are stable for many hours or even up to days rather than the expected microseconds. The limited gas diffusion through the water in the far field, the cooperative effect of nanobubble clusters, and the pinned contact line of the nanobubbles lead to the slow dissolution rate.

DOI: [10.1103/PhysRevLett.110.054501](https://doi.org/10.1103/PhysRevLett.110.054501)

PACS numbers: 47.55.db

Introduction.—Since their first prediction and discovery almost 20 years ago [1], intense research on surface nanobubbles has raised many questions about this intriguing and important phenomenon, which has great potential for various applications [2–5]. Surface nanobubbles have now been widely reported on various surfaces in contact with water employing various detection mechanisms like atomic force microscopy (AFM) and most recently also through direct optical visualization [6,7]. With all these different methods they are found to behave differently than regular macroscopic bubbles. Surface nanobubbles behave peculiarly in several ways: their contact angle is always much lower than expected from Young’s law [8,9]; they are stable against violent decompression [10]; and in particular they are stable for much longer than expected: For such small bubbles one would expect a lifetime of order μs , due to the high Laplace pressure inside the bubbles that drives the gas into the liquid. On this last question many explanations were proposed, ranging from contamination that shields or limits the diffusive outflux of gas [11] to a dynamic equilibrium situation where lost gas is replenished [12,13]. However, both theories are refuted by experimental evidence: the addition of surfactants does not influence the behavior of nanobubbles [14], and the circulatory gas flow required for the dynamic equilibrium theory is not measured in all experiments so it cannot be the stabilization mechanism [7,13]. In addition, a large problem with the dynamic equilibrium theory is that it requires some form of driving to satisfy the second law of thermodynamics, and its origin is unclear. In molecular dynamics, some local inflow near the contact line was indeed observed, but its strength was too weak to explain the stability of surface nanobubbles [15].

A different approach is therefore required, and in this Letter we provide an alternative explanation for the long lifetimes of surface nanobubbles. The theory relies only on classical, well-known, and proven continuum concepts such as diffusion and Henry’s law. Furthermore, the theory only uses confirmed nanobubble properties, namely the pinned contact line [16,17] of nanobubbles and the fact

that nanobubbles exist in relatively high coverage fractions at the liquid-solid interface [18,19]. No fitting or uncontrolled assumptions are required to obtain lifetimes that are consistent with experimental findings. The pinned contact line of surface nanobubbles has, until now, received little attention but it turns out to be crucial for long nanobubble lifetimes. The origin of the pinned contact lines is beyond the scope of this work and here we will only address the lifetime question of surface nanobubbles, which has been puzzling the community ever since the first discovery of surface nanobubbles [1].

The Letter is organized as follows. First, the theory is explained and the relevant equations are derived. Next, we solve the equations numerically and analytically. We vary several parameters to demonstrate the robustness of the long lifetimes of surface nanobubbles in varying experimental conditions. In addition, we apply the theory to the case of electrolytically generated nanobubbles and find that here also it is consistent with experimental results. We conclude with predictions from the theory that can straightforwardly be tested in experiments.

Theory.—We consider an infinitely large plate in contact with a liquid layer with thickness ℓ (Fig. 1). The liquid layer is in contact with the atmosphere at $z = \ell$ and the solid-liquid interface is located at $z = 0$. The solid-liquid interface is covered with nanobubbles with a number density (per area) of ρ ; hence the (average) spacing between neighboring nanobubbles is $\langle d_{\text{bub}} \rangle \approx 1/\sqrt{\rho}$. In experimental studies nanobubbles are always recovered in high coverage densities [18–21]. Assuming quasisteady diffusion, any variation of the dissolved gas concentration ϕ in the horizontal (x, y) direction due to nonuniform gas outflux decays as $\exp(-\pi z/d_{\text{bub}})$. Hence we can assume that for $\ell > 5\langle d_{\text{bub}} \rangle$ the diffusion of gas through the liquid layer is governed by the one-dimensional diffusion equation:

$$\frac{\partial \phi}{\partial t} = D \frac{\partial^2 \phi}{\partial z^2}, \quad z \in [0, \ell], \quad (1)$$

with D the diffusion constant of the gas in the ambient liquid and ϕ the (number) concentration of gas in the

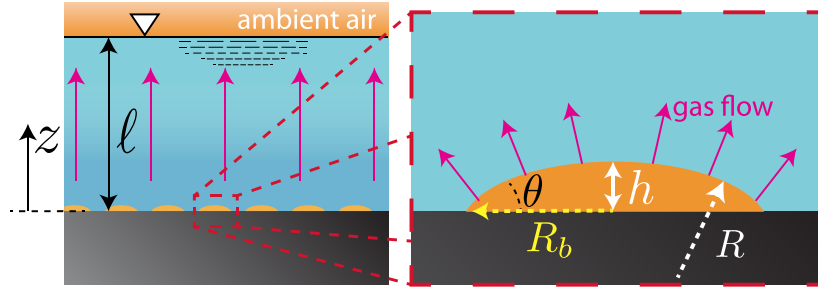


FIG. 1 (color online). Sketch of a liquid layer of thickness ℓ in contact with a solid (left). The top of the liquid is exposed to atmospheric conditions. At the solid-liquid interface nanobubbles are present with typical internal contact angle θ , height h , and radius of curvature R . They are not drawn to scale. The arrows indicate the gas flow direction. On the right a further enlargement of one nanobubble is shown.

liquid. The characteristic time scale for diffusion through the water layer is $\ell^2/D \sim 10^5$ s, which is similar to the lifetimes obtained in experiments. The vast difference (μ s vs days) compared to previous estimates originates in using ℓ as the relevant length scale instead of the bubble radius R ; i.e., we use the *far-field* length scale. Using R as the length scale is justified for a (free) bubble in an infinite medium. However, in the case of nanobubbles it is important to realize that gas has not left the system until it is released into the atmosphere, and hence ℓ is the relevant length scale as this is the distance the gas has to travel through the liquid from the bubble toward the atmosphere. This is also apparent in a thought experiment where we do not allow gas to leave the liquid into the atmosphere, for example, by putting the liquid drop in a closed container. Because the liquid is supersaturated with some gas that has left the bubble, and which cannot escape, an equilibrium is reached (described by Henry's law discussed later in this work) and the bubbles do not dissolve [22]. When opening the container this excess dissolved gas can be released into the ambient air, allowing the bubble to lose gas into the liquid. This “traffic jam effect” also plays a crucial role in the long nanobubble lifetimes.

We will now fully describe the boundary conditions for the above differential equation (1). They are given by Henry's law, which relates the gas concentration in the liquid to the gas pressure outside the liquid near the interfaces:

$$\phi(z=0, t) = \frac{p_{\text{bub}}[R(N(t))]}{k_H} \quad \text{and} \quad \phi(z=\ell, t) = \frac{p_{\text{atm}}}{k_H}. \quad (2)$$

Here, k_H is Henry's constant, p_{bub} the pressure inside the nanobubbles and p_{atm} the atmospheric pressure. $R(t)$ is the radius of curvature of the nanobubbles, which depends on time because the bubbles get flatter as they drain. In the case of a pinned contact line, the radius of curvature is related to the (internal) contact angle $\theta(t)$ by $R(t) = \frac{R_b}{\sin\theta(t)}$, where R_b is the base radius (cf. Fig. 1), which is constant

due to the pinned contact line. The (relative) pressure inside the bubbles $p_{\text{bub}}(t)$ is the Laplace pressure

$$p_{\text{bub}}(t) = p_{\text{atm}} + \frac{2\gamma}{R} = p_{\text{atm}} + \frac{2\gamma}{R_b} \sin\theta(t), \quad (3)$$

where γ is the liquid-vapor surface tension. For $\theta < 90^\circ$, which is the case for surface nanobubbles, the internal pressure thus decreases as θ decreases. This effect provides a negative feedback in the dissolution process, prolonging the lifetime of the nanobubbles. In this work we do not consider the effects of electrostatic effects on the internal pressure of surface nanobubbles, as electrostatic effects act to reduce the internal pressure and are therefore not a driving force but rather a stabilizing force. It is therefore possible that the derived lifetimes in this work (hours, days) are an underestimation of real lifetimes.

The (single) nanobubble gas content $N(t)$ decreases due to the diffusive flux of gas at $z=0$, which is the location at which gas is transferred from the nanobubbles ($z=0^-$) to the liquid ($z=0^+$). The diffusive flux is given by Fick's law $J = -D(\partial\phi/\partial z)$, thus

$$\frac{dN}{dt} = -\frac{J}{\rho} = \frac{D}{\rho} \frac{\partial\phi(z, t)}{\partial z} \Big|_{z=0}. \quad (4)$$

The factor ρ arises to convert the molecular flux per unit area of the substrate to the molecular flux per single surface nanobubble. Equation (4) immediately shows how a low nanobubble coverage ($\rho \approx 0$) corresponds to small global flux, $J = -\rho dN/dt$.

To evaluate the boundary condition at $z=0$ [Eq. (2)], we need to relate the number of atoms inside a nanobubble [Eq. (4)] to the geometrical shape of the bubble. To calculate the geometrical properties of a nanobubble containing N atoms of gas, we use the ideal gas law $p(\theta)V(\theta) = Nk_B T$ using the expression for the volume of a spherical cap $V(\theta) = \frac{\pi}{3}(R_b/\sin\theta)^3(2-3\cos\theta + \cos^3\theta)$. Here, k_B is Boltzmann's constant, T the temperature (assumed to be constant at 300 K), and θ the gas-side (internal) contact angle of the nanobubbles. This implicit equation can be solved numerically for $\theta(N)$. We can then calculate the

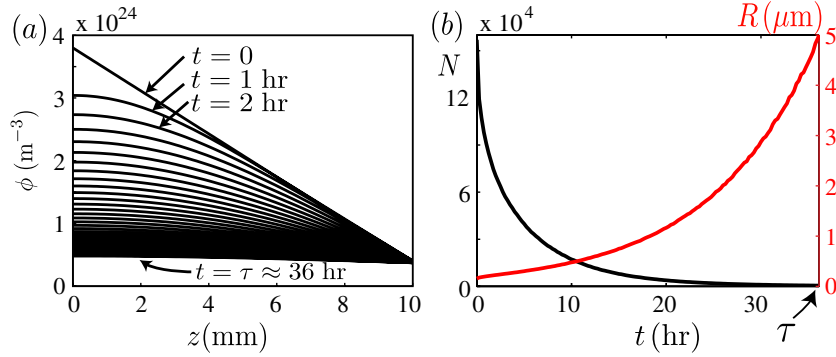


FIG. 2 (color online). Results of the calculations using the initial conditions from Eq. (5) and parameters described in the text. (a) Snapshots of the concentration profile at 1 h intervals. Because the bubbles are pinned, the radius of the curvature increases as the bubble drains, lowering the concentration at the bubble side ($z = 0$). (b) Evolution of the nanobubble gas content (black curve) and the radius of curvature of the liquid-gas interface R [red (gray) curve] as a function of time.

radius of curvature of the nanobubbles R , which gives us the internal bubble pressure [Eq. (3)]. Using this pressure, the boundary condition at $z = 0$ [Eq. (2)] can be evaluated, which closes our model. In the next section, we will solve these model equations numerically.

Numerical evaluation.—Due to the nontrivial boundary condition at $z = 0$ [Eq. (2)] we first solve the diffusion equation (1) numerically. The simulations were done for different initial conditions. Because the real initial conditions are unknown, we choose the two extremes between which we expect the real initial conditions. The first type of initial condition consists of a linear concentration profile, which allows the system to begin transporting gas from the bubbles immediately ($t = 0$),

$$\phi(z, t = 0) = \frac{p_{\text{bub}}(R_0) - p_{\text{atm}}}{k_H} \left(1 - \frac{z}{\ell}\right) + \frac{p_{\text{atm}}}{k_H}. \quad (5)$$

Here, R_0 indicates the initial radius of curvature of the nanobubbles. We choose R_0 such that it is equivalent to an initial contact angle $\theta_0 = 40^\circ$ for given base radius R_b .

The second type of initial condition assumes that the nanobubble formation procedure (ethanol-water exchange or replacing cold water with warm water [21]) supersaturates and mixes the water such that the concentration is uniform and equal to the concentration near the nanobubbles:

$$\phi(x, t = 0) = \frac{p_{\text{bub}}(R_0)}{k_H}. \quad (6)$$

The real initial concentration profile will most likely be something between (5) and (6): the ethanol-water exchange uniformly supersaturates the water but it takes the nanobubbles some time to form so some gas already drains into the atmosphere. As we will see, both initial concentration profiles produce long-living nanobubbles.

Results.—How long does a nanobubble survive according to this description? Using typical parameters that apply to experiments on surface nanobubbles [8]

($\bar{\rho} = 4 \times 10^{12} \text{ m}^{-2}$, $\ell = 10^{-2} \text{ m}$, $\gamma = 0.072 \text{ N/m}$, $D = 10^{-9} \text{ m}^2/\text{s}$, $k_H = 2.6 \times 10^{-19} \text{ Pa} \cdot \text{m}$, and $T = 300 \text{ K}$) and the initial condition [Eq. (5)] we obtain the results shown in Fig. 2. Figure 2(a) shows hourly snapshots of the concentration profile $\phi(z)$. From these curves it is apparent that the transport of gas away from the bubble is limited by the diffusion rate of the gas through water far away from the bubble. This leads to an almost flat (zero-slope) concentration profile near the bubble through which the diffusive gas flux is very small. Figure 2(b) [red (gray) curve] shows the radius of curvature of the spherical cap R as a function of time. This radius of curvature increases (due to the pinned contact line), which lowers the internal gas pressure [Eq. (3)], enhancing the lifetime of the nanobubbles. Finally, Fig. 2(b) (black curve) shows the amount of particles contained inside an individual nanobubble through time. Here we see that a typical nanobubble that starts out with over 100 000 atoms and ends up with just over 500 atoms after 36 h.

As a criterion for bubble dissolution we choose a critical bubble height of $h^* = 1 \text{ nm}$, after which it may no longer be appropriate to use continuum physics, and also effects such as the disjoining pressure start to dominate the pressure inside the bubble rather than solely the Laplace pressure. From molecular dynamics it is known that continuum models (e.g., Navier-Stokes, diffusion equation, Henry's law) are valid down to the nanometer scale [15,22]. Using the same criterion we find that above bubble is stable for 36 h, which is 10 orders of magnitude longer than previously thought and in agreement with experimental findings and the expected time scale ℓ^2/D .

Analytic solution.—The concentration profiles in Fig. 2 suggest that the boundary condition at $z = 0$ is of Neumann type, $\partial\phi/\partial z|_{z=0} = 0$. Taking the time derivative of the boundary condition at $z = 0$ [Eq. (2)] and substituting Eq. (4) into the result we obtain

$$\frac{\partial\phi}{\partial z} \Big|_{z=0} = \frac{\rho}{D} \frac{d\phi}{dN} \frac{\partial\phi}{\partial t} \Big|_{z=0}. \quad (7)$$

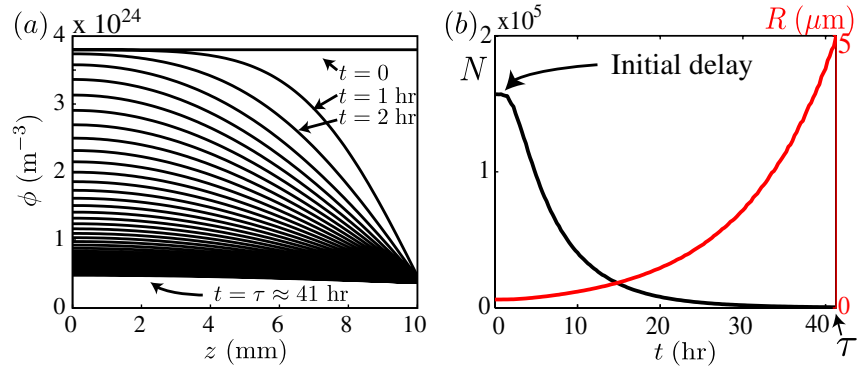


FIG. 3 (color online). Numerical results for the initial conditions [Eq. (6)]. (a) Hourly snapshots of the concentration profile. Due to the initial conditions, some gas that is initially dissolved in the liquid first has to drain to the atmosphere until a concentration gradient exists near the bubble. As compared to the linear profile case (Fig. 2) the bubbles gain an additional few hours of lifetime because of this. (b) Evolution of the nanobubble gas content and the radius of curvature of the surface nanobubbles.

Filling in representative values for the quantities we find that the concentration gradient at $z = 0$ is over 5 orders of magnitude smaller than the typical global concentration gradient ($\approx \hat{\phi}/\ell$), with $\hat{\phi} = \phi - \phi_{\text{atm}}$. This means that the boundary condition for the gradient at $z = 0$ can indeed be considered to be approximately zero. For zero gradient the analytic solution is $\hat{\phi}(z, t) = \hat{\phi}_{\text{bub},0} \exp(-\pi^2 Dt/(4\ell^2)) \cos(\pi z/(2\ell)) + \hat{\phi}_{\text{transient}}(t)$. The exact form of $\hat{\phi}_{\text{transient}}$ depends on the initial conditions but declines quickly. A remarkable feature of this result is that $\hat{\phi}(z, t)$ only depends on D and ℓ and is completely independent of ρ and γ . Of course, ρ must be high enough to be able to consider the system as one dimensional. Similarly, the fraction $\rho/(Dd\phi/dN)$ must be low enough such that the local gradient at $z = 0$ [Eq. (7)] is small compared to the global gradient.

Varying initial conditions.—How does the initial concentration profile affect the lifetime of the nanobubbles? During the ethanol-water exchange procedure that is most commonly used to generate nanobubbles experimentally, ethanol is flushed away with clean water. It is therefore likely that the initial gas concentration profile is uniform in z , due to mixing. We redid the same calculations as before, using an uniform initial concentration profile, and the results are plotted in Fig. 3. We observe very similar concentration profiles as before, except for small times where the influence of the initial conditions is still felt. As can be observed in Fig. 3(b), it takes 2–3 h before the bubbles “feel” the influence of the ambient air and start to dissolve. This means that during these first hours, the bubbles barely shrink as the (global) concentration gradient near the bubbles is close to zero.

Robustness of the results.—How robust are the nanobubble lifetimes against variations in the experimental system? By changing γ and ℓ in the numerical calculation, we verify the result from the analytical solution to the diffusion equation for which it holds that the diffusion profile evolution only depends on D and ℓ .

First, we look at the surface tension γ . Most often an ethanol-water exchange procedure is applied to form nanobubbles. This method introduces contamination into the system, which lowers the surface tension. It is therefore important to understand the influence of γ on the nanobubble lifetime. We find that surface tension does not play any role in the dissolution time of nanobubbles. This result remains counterintuitive as surface tension is the driving force for nanobubble dissolution. Indeed, a higher surface tension increases the Laplace pressure [Eq. (3)], thus increasing the driving that leads to dissolution. However, it also increases the gas content inside the bubbles. This denser reservoir requires a larger flux to drain in the same time. Both effects scale linearly with γ ; hence, they cancel.

In previous studies, the liquid height ℓ has never been considered as a parameter that affects nanobubble lifetimes. Based on the analytical solution presented before we expect that $\tau \sim \ell^2/D$, which is indeed exactly recovered from the numerical calculations. This indicates that the liquid cell size (and geometry) is very important to the lifetime of nanobubbles: the amount of liquid the gas has to travel through determines the time scale of the nanobubble lifetime. ℓ is easy to vary, we suggest performing corresponding experiments to test our prediction.

Electrolysis.—How do nanobubbles behave according to this description when gas is generated at the solid-liquid interface (e.g., by electrolysis [16,23])? A rough estimate based on the values cited in Ref. [16] gives a constant influx of order $\sim 10^5$ molecules per bubble per second. For an equilibrium to exist (the bubbles neither grow or shrink) the diffusive flux away from the bubble must then be equal to this influx due to electrolysis, hence $\frac{D}{\rho} \hat{\phi}(z=0)/\ell = 10^5 \text{ s}^{-1}$. This corresponds to a nanobubble contact angle of $\theta = 49^\circ$ and nanobubble content $N = 2 \times 10^5$. Interestingly, this means that the bubble contents are refreshed every two seconds. This only highlights the fact that nanobubbles are not static: without driving (such as electrolysis) they dissolve, whereas with driving the gas

atoms inside the bubble are replaced every couple of seconds.

Conclusion.—We have modeled the gas flow from nanobubbles through the liquid to the atmosphere to study the lifetime of surface nanobubbles. We find that nanobubbles are not stable, but dissolve by diffusion. However, due to their pinned contact lines and because the gas has to diffuse toward the atmosphere, they dissolve on a much longer time scale than free bubbles in an infinite liquid. This last point (diffusion through a relatively thick layer of liquid) explains why previous molecular dynamics results could not recover long nanobubble lifetimes: the system size in molecular dynamics is limited to several tens of nanometers, resulting in lifetimes of order 100 ns, consistent with our findings in Ref. [15]. Using the correct length scales ($\ell \sim 1\text{--}10$ mm), we find that surface nanobubbles can easily survive in excess of a day, an increase of 10 orders of magnitudes as compared to previous estimates of μs . The results from the experiment where electrolysis is used corroborate the results in this Letter: a nonzero current is measured, meaning that gas is continuously formed at the substrate. We find that the gas flux induced by this current leads to nanobubbles with $\theta = 46^\circ$, consistent with the experimental results of Ref. [16].

J.H. Snoeijer, H. Gelderblom, and X.H. Zhang are gratefully acknowledged for discussions. This work is part of the research programme of the Foundation for Fundamental Research on Matter (FOM), which is part of the Netherlands Organisation for Scientific Research (NWO).

-
- [1] J. Parker, P. Claesson, and P. Attard, *J. Phys. Chem.* **98**, 8468 (1994).
 [2] M. A. Hampton and A. V. Nguyen, *Adv. Colloid Interface Sci.* **154**, 30 (2010).

- [3] J. R. T. Seddon and D. Lohse, *J. Phys. Condens. Matter* **23**, 133001 (2011).
 [4] V. S. J. Craig, *Soft Matter* **7**, 40 (2011).
 [5] J. R. T. Seddon, D. Lohse, W. A. Ducker, and V. S. J. Craig, *ChemPhysChem* **13**, 2179 (2012).
 [6] S. Karpitschka, E. Dietrich, J. R. T. Seddon, H. J. W. Zandvliet, D. Lohse, and H. Riegler, *Phys. Rev. Lett.* **109**, 066102 (2012).
 [7] C. U. Chan and C.-D. Ohl, *Phys. Rev. Lett.*, **109**, 174501 (2012).
 [8] B. M. Borkent, S. de Beer, F. Mugele, and D. Lohse, *Langmuir* **26**, 260 (2010).
 [9] X. H. Zhang, N. Maeda, and V. S. J. Craig, *Langmuir* **22**, 5025 (2006).
 [10] B. M. Borkent, S. M. Dammer, H. Schönherr, G. J. Vancso, and D. Lohse, *Phys. Rev. Lett.* **98**, 204502 (2007).
 [11] W. A. Ducker, *Langmuir* **25**, 8907 (2009).
 [12] M. P. Brenner and D. Lohse, *Phys. Rev. Lett.* **101**, 214505 (2008).
 [13] J. R. T. Seddon, H. J. W. Zandvliet, and D. Lohse, *Phys. Rev. Lett.* **107**, 116101 (2011).
 [14] X. Zhang, M. H. Uddin, H. Yang, G. Toikka, W. Ducker, and N. Maeda, *Langmuir* **28**, 10471 (2012).
 [15] J. H. Weijs, J. H. Snoeijer, and D. Lohse, *Phys. Rev. Lett.* **108**, 104501 (2012).
 [16] S. Yang, P. Tsai, E. S. Kooij, A. Prosperetti, H. J. W. Zandvliet, and D. Lohse, *Langmuir* **25**, 1466 (2009).
 [17] X. Zhang, D. Y. C. Chan, D. Wang, and N. Maeda, *Langmuir* (in press).
 [18] S. Yang, S. M. Dammer, N. Bremond, H. J. W. Zandvliet, E. S. Kooij, and D. Lohse, *Langmuir* **23**, 7072 (2007).
 [19] S. Yang, E. S. Kooij, B. Poelsema, D. Lohse, and H. J. W. Zandvliet, *Europhys. Lett.* **81**, 64006 (2008).
 [20] J. W. G. Tyrrell and P. Attard, *Langmuir* **18**, 160 (2002).
 [21] X. H. Zhang, X. Zhang, J. Sun, Z. Zhang, G. Li, H. Fang, X. Xiao, X. Zeng, and J. Hu, *Langmuir* **23**, 1778 (2007).
 [22] J. H. Weijs, J. R. T. Seddon, and D. Lohse, *ChemPhysChem* **13**, 2197 (2012).
 [23] L. Zhang, Y. Zhang, X. Zhang, Z. Li, G. Shen, M. Ye, C. Fan, H. Fang, and J. Hu, *Langmuir* **22**, 8109 (2006).